Original Article

Dynamic biomarker and imaging changes from a phase II study of pre- and post-surgical sunitinib

Sarah J. Welsh[1,2,3] (iD), Nicola Thompson[1], Anne Warren[3,4], Andrew N. Priest[5] (iD), Tristan Barrett[3,5], Stephan Ursprung[3,5], Ferdia A. Gallagher[3,5], Fulvio Zaccagna[5], Grant D. Stewart[2,3] (iD), Kate M. Fife[1,3] (iD), Athena Matakidou[1,3,6], Andrea J. Machin[1], Wendi Qian[1], Victoria Ingleson[1], Jean Mullin[1], Antony C. P. Riddick[2,3], James N. Armitage[2,3], Stephen Connolly[7] and Timothy G. Q. Eisen[1,3,8]

[1]*Department of Oncology, Cambridge University Hospitals NHS Foundation Trust*, [2]*Department of Surgery, Cambridge University Hospitals NHS Foundation Trust*, [3]*Cancer Research UK Cambridge Centre Urological Malignancies Programme, University of Cambridge*, [4]*Department of Pathology, Cambridge University Hospitals NHS Foundation Trust*, [5]*Department of Radiology, University of Cambridge, Cambridge*, [6]*GlaxoSmithKline, Brentford, UK*, [7]*Department of Urology, Mater Misericordiae University Hospital, University College Dublin, Dublin 7, Ireland, and* [8]*Roche, Welwyn Garden City, UK*

Objective

To explore translational biological and imaging biomarkers for sunitinib treatment before and after debulking nephrectomy in the NeoSun (European Union Drug Regulating Authorities Clinical Trials Database [EudraCT] number: 2005-004502-82) single-centre, single-arm, single-agent, Phase II trial.

Patients and Methods

Treatment-naïve patients with metastatic renal cell carcinoma (mRCC) received 50 mg once daily sunitinib for 12 days pre-surgically, then post-surgery on 4 week-on, 2 week-off, repeating 6-week cycles until disease progression in a single arm phase II trial. Structural and dynamic contrast-enhanced magnet resonance imaging (DCE-MRI) and research blood sampling were performed at baseline and after 12 days. Computed tomography imaging was performed at baseline and post-surgery then every two cycles. The primary endpoint was objective response rate (Response Evaluation Criteria In Solid Tumors [RECIST]) excluding the resected kidney. Secondary endpoints included changes in DCE-MRI of the tumour following pre-surgery sunitinib, overall survival (OS), progression-free survival (PFS), response duration, surgical morbidity/mortality, and toxicity. Translational and imaging endpoints were exploratory.

Results

A total of 14 patients received pre-surgery sunitinib, 71% (10/14) took the planned 12 doses. All underwent nephrectomy, and 13 recommenced sunitinib postoperatively. In all, 58.3% (seven of 12) of patients achieved partial or complete response (PR or CR) (95% confidence interval 27.7–84.8%). The median OS was 33.7 months and median PFS was 15.7 months. Amongst those achieving a PR or CR, the median response duration was 8.7 months. No unexpected surgical complications, sunitinib-related toxicities, or surgical delays occurred. Within the translational endpoints, pre-surgical sunitinib significantly increased necrosis, and reduced cluster of differentiation-31 (CD31), Ki67, circulating vascular endothelial growth factor-C (VEGF-C), and transfer constant (K^{Trans}, measured using DCE-MRI; all $P < 0.05$). There was a trend for improved OS in patients with high baseline plasma VEGF-C expression ($P = 0.02$). Reduction in radiological tumour volume after pre-surgical sunitinib correlated with high percentage of solid tumour components at baseline (Spearman's coefficient $\rho = 0.69$, $P = 0.02$). Conversely, the percentage tumour volume reduction correlated with lower baseline percentage necrosis (coefficient = −0.51, $P = 0.03$).

Conclusion

Neoadjuvant studies such as the NeoSun can safely and effectively explore translational biological and imaging endpoints.

Keywords

neoadjuvant therapy, renal cell carcinoma, nephrectomy, sunitinib

Introduction

Renal cell carcinoma (RCC) accounts for ~3% of adult malignancies [1]. Antiangiogenic therapies have improved the prognosis of patients with metastatic RCC (mRCC), and tyrosine kinase inhibitors (TKIs) such as sunitinib, may now be integrated with surgical treatment and other systemic treatments such as immunotherapy to optimise outcomes for patients with RCC [2,3].

Several trials of neoadjuvant therapy for RCC and mRCC have recently been completed or are ongoing [4–7] (Table 1), and there is increasing evidence of the safety, effectiveness and utility of this approach [4,8]. Recently, the Cancer du Rein Metastatique Nephrectomie et Antiangiogéniques (CARMENA) and Immediate Surgery or Surgery After Sunitinib Malate in Treating Patients With Metastatic Kidney Cancer (SURTIME) [2,4] trials have shown that patients with International Metastatic RCC Database Consortium (IMDC) intermediate- and high-risk RCCs are best treated with up-front TKIs rather than up-front cytoreductive nephrectomy. It is hypothesised that this approach allows the biology of the disease to be unveiled, sparing patients with aggressive RCCs from surgery and its associated morbidity [9].

One purported advantage of neoadjuvant therapy in the context of mRCC is to reduce tumour volume and facilitate surgical resection, and in cases of caval tumour thrombus (TT) this may be particularly beneficial to potentially down-stage the TT to facilitate less extensive surgery. This is being explored currently in the NAXIVA trial (NCT03494816, a study of preoperative axitinib to reduce extent of tumour venous thrombus in renal cancer with venous invasion). Neoadjuvant treatment may also allow imaging and molecular assessment of response to guide future systemic therapy.

In the present study, sunitinib was chosen as the targeted agent because it was the most extensively investigated targeted agent at the time of the study, is approved as first-line treatment for mRCC, and is considered a suitable agent for neoadjuvant treatment given its ability to shrink primary tumours [2,10]. A short duration of preoperative sunitinib was planned to devascularise the tumour without having a major impact on tumour volume. The objectives of the present study were to evaluate the treatment's efficacy, safety, and tolerability, and to identify potential markers of response using imaging and translational studies.

Patients and Methods

Study Design

The NeoSun (European Union Drug Regulating Authorities Clinical Trials Database [EudraCT] number: 2005-004502-82) was a single-centre, single-arm, single-agent, Phase II trial. National research ethics committee approval was obtained (REC ref: 09/HO304/69) and written informed consent was provided by the study participants. The original design was a two-stage study with 18 patients in the first stage and 17 patients in the second stage. The study was terminated due to slow recruitment in December 2013 after 16 patients had been recruited. Data collection continued until December 2015. The trial schema is shown in Fig. S1.

Trial Treatment

Sunitinib was administered orally at 50 mg once daily starting 14 days before nephrectomy was scheduled and taken for 12 days, with a 2-day break before surgery. Patients were recommenced sunitinib when medically fit (minimum 15 days postoperatively), continuing on a 4-week on, 2-week off repeating cycle. This was continued until progressive disease

Table 1 Summary of other neoadjuvant studies.

Drug	N	RN/PN	Overall PR, n (%)	Surgical safety	Biomarker study	Pre-surgical course duration, weeks
Pazopanib [13]	104	43/22	13%	Y	VEGFR2, c-Met, PD-L1, CD8	12–14
Pazopanib [20]	25	5/20	10 (36)	N/A	N/A	8–16
Sunitinib [5]	72	13/49	15 (19)	Y	N/A	6–12
Axitinib [16]	24	19/5	11 (45.8)	Y	N/A	12
Sunitinib or Sorafenib [21]	14	14/0	8 (57)	N/A	N/A	6–30
Sunitinib or Sorafenib [22]	14	11/0	2 (14.3)	Y*	N/A	3–48
Sunitinib [6]	28	13/0	7 (24.1)	Y	N/A	Until resectability
Sunitinib [23]	20	12/8	1 (5)	Y	N/A	12
Sunitinib [24]	12	0/12	4 (28.6)	Y	N/A	8
Sunitinib [7]	19	4/0	3 (16)	Y	N/A	Until resectability (min. 12)
Sunitinib vs immediate nephrectomy [4]	49 vs 50	N/A	N/A	Y	N/A	18
Sunitinib [14]	66	47/0	13 (20)	Y	DW MRI	12–16
Sunitinib [17]	32	20/0	9 (33)*	N/A	Panel of blood based angiogenic biomarkers	12

c-Met, mesenchymal–epithelial transition factor; DW MRI, diffusion-weighted MRI; PD-L1; programmed death-ligand 1; PN, partial nephrectomy; RN, radical nephrectomy. Surgical safety as assessed by the study authors. *Change in primary renal tumour size of >10%.

(Response Evaluation Criteria In Solid Tumors [RECIST] version 1.1 [11]) or unacceptable toxicity (assessed by the National Cancer Institute-Common Terminology Criteria for Adverse Events [NCI-CTCAE] version 4·0). CT scans were performed every 12 weeks until progression.

Study Objectives

Primary objective:

- To determine the anti-cancer activity of sunitinib when given before and after nephrectomy to previously untreated patients with mRCC.

Secondary objectives:

- To describe the toxic effects of sunitinib given before and after nephrectomy to previously untreated patients with mRCC.
- To evaluate, pathologically, evidence of sunitinib activity in the primary RCC lesion.
- To correlate pathological and clinical response.
- To correlate changes in blood and tumour biomarkers with treatment response.
- To evaluate changes in structural and dynamic contrast-enhanced MRI (DCE-MRI) of the tumour before and after 12 days of Sunitinib therapy.

Exploratory objectives:

- To identify molecular and imaging biomarkers of response.

Study Patients

Between October 2010 and January 2014, 22 patients were screened for eligibility, and 16 were enrolled. Patient characteristics are shown in Table 2. Key inclusion criteria were histopathologically confirmed clear cell RCC with metastases, judged by the treating clinician to potentially derive benefit from sunitinib. Key exclusion criteria included previous treatment for mRCC and contra-indication to MRI. Eligible patients underwent screening procedures before treatment with sunitinib.

Cycle 2 Day 1 (C2D1) procedures took place ≥15 days postoperatively and the patient re-started study drug that day. At the end of the study or at withdrawal for toxicity/progression or other reasons, patient care and follow-up was as per local standard procedure. Patients who withdrew for reasons other than disease progression were assessed (including RECIST) at least 3-monthly. Survival data for all patients were provided 3-monthly.

Surgery

The operating surgeon decided on the surgical approach. Transfusion thresholds were at the discretion of the surgical team (typically haemoglobin <80 g/L unless a history of

cardiovascular disease). Complications were recorded according to the Clavien–Dindo classification [12].

Evaluation of Response

Imaging (Including Imaging Biomarker Assessments)

The RECIST version 1.1 [11] was used to assess tumour response using contrast-enhanced CT scans (thorax, abdomen, and pelvis), performed at C1D1 (baseline), on re-starting treatment after surgery (C2D1), then 12-weekly until disease progression. For endpoints based on RECIST, measurements excluded the primary RCC target lesion (as this was resected) and included longitudinal measurements after surgery. MRI was performed at baseline and C1D12, including multiplanar anatomical T_1 and T_2-weighted imaging, and physiological sequences including DCE-MRI using a 1.5-T Discovery MR450 system (GE Healthcare, Waukesha, WI, USA) using an eight-channel cardiac array coil.

The T_2-weighted structural images were acquired in axial, sagittal and coronal orientations using a respiratory-triggered fast-recovery Fast Spin-Echo pulse sequence, with these parameters: echo time (TE) 48–69 ms; repetition time (TR) 1 breath; echo train length (ETL) 10–13; field of view (FoV) 35×35 cm^2; slice thickness/gap = 4/1 mm; acquisition matrix 320×224; 2 Nex with no phase-wrap to remove aliasing. The T_1-weighted structural images were acquired using a breath-hold two-dimensional (2D) fast spoiled gradient-echo (FSPGR) sequence with these parameters: TE 4.8 ms; TR 139 ms; flip angle 70°; FoV 35×35 cm^2; slice thickness/gap 4/1 mm; acquisition matrix 256×256; 0.75 Nex (partial Fourier); parallel imaging (Array coil Spatial Sensitivity Encoding [ASSET]) factor 2.

The DCE-MRI imaging data were acquired using a three-dimensional (3D) FSPGR sequence in coronal oblique orientation with the following parameters: TE 1.6 ms; TR 3.9 ms; flip angle 18°; FoV 35×35 cm^2; slice thickness 5 mm; acquisition matrix $160 \times 160 \times 20$–30; receiver bandwidth ±41.67 kHz; 0.5 Nex (elliptical k-space coverage); parallel imaging (ASSET) factor 2; temporal resolution 4.3–6.4 s; 94–140 dynamic phases; total scan time 10 min. The number of slices (and consequently the temporal resolution) was varied in order to image the entire tumour volume. 0.1 mmol/kg of gadolinium-tetraazacyclododecane tetraacetic acid (Gd-DOTA; Dotarem, Guerbet, Paris, France) was administered during the dynamic series at a flowrate of 3 mL/s.

The DCE-MRI acquisition was preceded by acquisition of T_1 mapping data using a multiple flip-angle FSPGR technique (flip angles 1°, 3°, 5°, 10°, 15°, 20°) with 1 Nex; no parallel imaging; scan time 12.5 s (breath-hold) for each flip angle,

Table 2 Summary of baseline patient characteristics.

Characteristic	Median or *n*	Range (min–max) or %
Age, years	60	50–73
Gender (male/female)	15/1	94/6
Pre-existing comorbidities		
Coronary heart disease	1	6.25
Diabetes	1	6.25
Hypertension	3	18.75
Others (asthma, osteoarthritis, gout, kidney stones, skin lesion, depression, varicose veins, gastritis, umbilical hernia, disk prolapse, benign prostatic hyperplasia)	1 each	6.25
Eastern Cooperative Oncology Group (ECOG) score		
0	12	75
1	4	25
Memorial Sloan-Kettering Cancer Center (MSKCC) risk		
Favourable	1	6.25
Intermediate	11	68.75
Poor	4	25
Number of target lesions per subject at baseline		
2	7	44
3	7	44
4	2	13
Sites of target lesions	43	
Lung	13	30
Liver	1	2
Lymph nodes	8	19
Other sites	21	49
Size of lesions (measured on baseline CT)		
Mean/median diameter – primary lesion, cm	11.2/11.7	7.3–15.7
Mean/median diameter – sum of target lesions (including primary), cm	14.8/14.8	8.2–24.3
Mean/median diameter – sum of target lesions (excluding primary), cm	4.67/3.10	1.0–12.0
Sites of non-target lesions	20	
Lung	12	60
Liver	1	5
Renal tumour	1	5
Lymph nodes	4	20
Bones	2	10
Pathological stage		
pT1b	1	6.25
pT3a	13	81.25
pT3b	2	12.5
pNx	2	12.5
pN0	10	62.5
pN1	4	25
Fuhrman grade		
2	3	18.75
3	8	50
4	5	31.25
Laboratory results		
Leukocytes, $\times 10^9$/L	7.3	4.6–9.5
Haemoglobin, g/L	119	82–172
Platelets, $\times 10^9$/L	279.5	137–468
Calcium, mmol/L	2.4	2.0–2.9
Adjuvant therapy	13	92.9

with the other parameters the same as for the DCE-MRI series.

The T_1 mapping and DCE-MRI data were processed in MIStar (Apollo Medical Imaging Technology, Melbourne, Victoria, Australia). Each dataset was pre-processed using a 3×3 median filter. The T_1 mapping and DCE datasets were co-registered both within and between the datasets to remove (as far as possible) spatial mis-registrations caused by motion. Registration used a mutual information metric to cope with the variations in contrast between images within the DCE and T_1 map series. Where possible a 2D rigid-body registration was applied focussed on the region of interest. In some cases the 2D approach failed and instead a 3D rigid-body registration used; occasionally neither approach worked, and a deformable registration was necessary. Registration was performed as a batch, with each image registered pairwise to the same reference image where possible, although in some cases a separate reference image was used for specific phases that failed to register correctly. In all cases the images were

viewed as a movie after registration to confirm the registration success before proceeding to the DCE analysis. Together the T_1 mapping and DCE datasets were used to calculate dynamic maps of Gd concentration, which was fitted using the Tofts model 10508281 with a population average arterial input function to calculate maps of the transfer constant K^{trans} [25].

Normal kidney, whole tumour, cystic/necrotic and solid tumour regions of interest (ROIs) were outlined by an experienced radiologist using manual segmentation using ImageSetViewer Software, version 1.7 (University Health Network, Toronto, ON, Canada) in order to generate and compare 3D renderings of tumours and surrounding normal tissues before and after treatment. Segmentation was performed on the coronal T_2-weighted FRFSE sequence, these outlines were then directly transposed onto the coronal-oblique DCE early post-contrast sequences using the ImageSetViewer Software, with minor manual adjustment or ROIs being performed as required. The segmentation was undertaken blinded to the clinical outcome and RECIST measurements.

Pathological Response (Including Pathology-Based Biomarker Assessments)

Image-guided tumour core biopsies were taken before patients started treatment. Tumour and normal kidney punch biopsies were also taken by pathologists from normal and tumour regions from nephrectomy tissue. Tissue was fixed and paraffin-embedded, then 3-μm serial sections were mounted on Snowcoat X-tra slides (Surgipath, Richmond, IL, USA). Sections were dewaxed in xylene (2 × 10 min), rehydrated (100% ethanol 2 × 5 min, 70% ethanol 1 × 5 min) through to tap water (1 × 5 min), stained in Harris haematoxylin (Leica 3801560BBE 1 × 2 min; Leica Biosystems Newcastle Ltd., Newcastle upon Tyne, UK), washed in tap water (1 × 5 min), acid dipped (2% Acid Alcohol 1 × 20 s), washed in tap water (1 × 5 min), stained in 1% aqueous eosin (Leica 3801590BBE 1 × 7 min) and then dehydrated (50% ethanol with 0.1% Tween 1 × 20 s, 70% ethanol with 0.1% Tween 1 × 20 s, 100% ethanol 1 × 30 s, 100% ethanol 1 × 1 min), cleared in xylene (2 × 5 min) and cover-slipped on an automated cover-slipper (Leica CV5030).

Immunohistochemistry (IHC) was performed on formalin-fixed paraffin-embedded tissue samples using a Leica Autostainer XL (ST5010). Substitution of the primary antibody with antibody diluent was used as a negative control. Antigen/antibody complexes were detected using the Envision system (Dako, Glostrup, Denmark) according to the manufacturer's instructions. Sections were counterstained with Harris haematoxylin (Cell Path) for 30 s, dehydrated in graded ethanol washes as above, and mounted in dibutyl

phthalate in xylene (DPX; Lamb, London, UK). Antibodies used were: cluster of differentiation-31 (CD31, 10 μg/mL; BD Biosciences, San Jose, CA, USA), Ki67 (1:1000; Bethyl Laboratories, Montgomery, TX, USA) cleaved caspase 3 (1:200; Cell Signaling Technology, Inc., Danvers, MA, USA). Slides were cover-slipped with Pertex (Leica) on 2 × Thermo ClearVue machines. Microvessel density (CD31) and Ki67 were quantified using a computerised image-analysis system (ARIOL, Applied Imaging, Genetix) using visually-trained parameters. The percentage of total tumour necrosis was determined by a pathologist using randomly selected haematoxylin and eosin sections.

Blood-Based Biomarker Assessments (vascular endothelial growth factor [VEGF])

Blood samples were collected on C1D1 and C1D12. Whole blood (9 mL) was collected by standard venesection into Vacutainer tubes (Becton Dickinson, Franklin Lakes, NJ, USA). Blood was allowed to clot by leaving it undisturbed at room temperature for 30 min. Samples were then centrifuged at 1500*g* for 10 min in a refrigerated centrifuge. Serum was collected and stored in 0.5 mL aliquots at −80 °C until assay. Immediately before assay, samples were thawed on ice and VEGF-A and VEGF-C proteins were measured by enzyme-linked immunosorbent assay (ELISA; Human VEGF-A and VEGF-C-ELISA kits; R&D Systems, Minneapolis, MN, USA), according to the manufacturer's instructions.

Statistical Analysis

Statistical analyses were mainly descriptive on clinical endpoints (Appendix S1).

Results
Patient Characteristics and Outcomes

Demographics

A total of 16 subjects were registered between 29 Oct 2010 and 15 Jan 2014; however, two patients withdrew before starting treatment. Patient characteristics are shown in Table 2.

Treatment

A Consolidated Standards of Reporting Trials (CONSORT) diagram is shown in Fig. S2. A total of 14 patients received pre-surgery cycle 1, with 71% (10/14) taking the planned 12 doses. All 14 patients underwent total nephrectomy and 13 recommended sunitinib postoperatively. The mean (range) number of post-surgery cycles received was 12 (2–22). There was no correlation between number of pre-surgery doses and any of the primary or secondary endpoints.

Clinical Outcomes

The primary endpoint was not reached due to premature closure of the trial, but clinical outcome data are described in the Supplementary Results in Appendix S1.

Safety and Toxicity of Sunitinib

Safety and toxicity of sunitinib was consistent with previously reported outcomes (Table S1). No unexpected surgical outcomes or complications were reported (Table S2). No surgical delays occurred.

Imaging Endpoints

Changes in DCE-MRI of the primary tumour were assessed before and after 12 days of sunitinib therapy (Fig. 1). A total of 12 patients were evaluable and representative images are shown in Fig. 1A. All patients had RECIST-defined stable disease in their primary tumour after 12 days of sunitinib, measured using MRI. The mean (range) percentage change in primary tumour size measured using MRI was −6.01 (−16.6 to +4.3)%, with three patients having a change of >10% despite the short treatment duration. The mean total tumour volume reduction was 20.0% (90–1213 mL; $P = 0.001$) and the mean total volume reduction within the solid portions of the tumour was 24% from a mean (range) of 388 (99–903) to 295 (81–749) mL ($P < 0.001$). A slight increase in the mean

volume of the normal ipsilateral kidney by 5.5 mL (3%; $P = 0.039$) was observed after 12 days of sunitinib therapy but is unlikely to be clinically significant and lies within the margin of measurement error. MRI derived K^{trans} (a measure of capillary permeability) also significantly reduced within the solid portions of the tumour by a mean of 28% ($P = 0.006$; Fig. 1B). Additionally, patients with a higher percentage of solid tumour components at baseline showed a greater reduction in overall tumour volume (Spearman rank correlation coefficient $\rho = 0.69$, $P = 0.02$). There was some indication (correlation coefficient $\rho = 0.4$, $P = 0.15$) a higher baseline K^{trans} in the solid tumour correlated to a larger solid tumour volume reduction, within the small sample size. However, none of these parameters correlated with OS or PFS or overall response rate (ORR).

Pathological Endpoints

Pathological Response

A total of 13/14 patients had evaluable tissue for analysis of necrosis using IHC before treatment with 12 days of sunitinib therapy, and 14/14 patients had evaluable tissue after therapy. The mean (range) necrosis before and after treatment was significantly increased from 9.6 (0–60)% to 29.6 (0–75)%, respectively ($P = 0.024$; Fig. 2A). The mean (range) change in necrosis between time points was 20.4 (0–70)%. Neither of

Fig. 1 (A) This figure summarises the typical response patterns observed on imaging following 12 days (2W) of pre-surgical sunitinib treatment. Patient one presented with a mainly solid tumour that showed a clear reduction in tumour volume at 2 weeks. The tumour is outlined in red on the T_2-weighted (T_2w) morphological MRI sequence. A reduction in tumour perfusion and blood vessel permeability is apparent on the K^{Trans} map. The relative composition of the tumour and the reduction in tumour volume is visible in 3D-renderings with the normal kidney in light blue, the solid tumour in red, and the cystic and necrotic tumour compartment in blue. In contrast, patient two presented with a poorly perfused, mainly necrotic tumour and only experienced a very modest reduction in tumour volume and perfusion during the pre-surgical treatment. (B) Significant differences were seen in K^{Trans} within the whole tumour, in solid areas of the tumour, and in normal kidney consistent with sunitinib's mechanism of action.
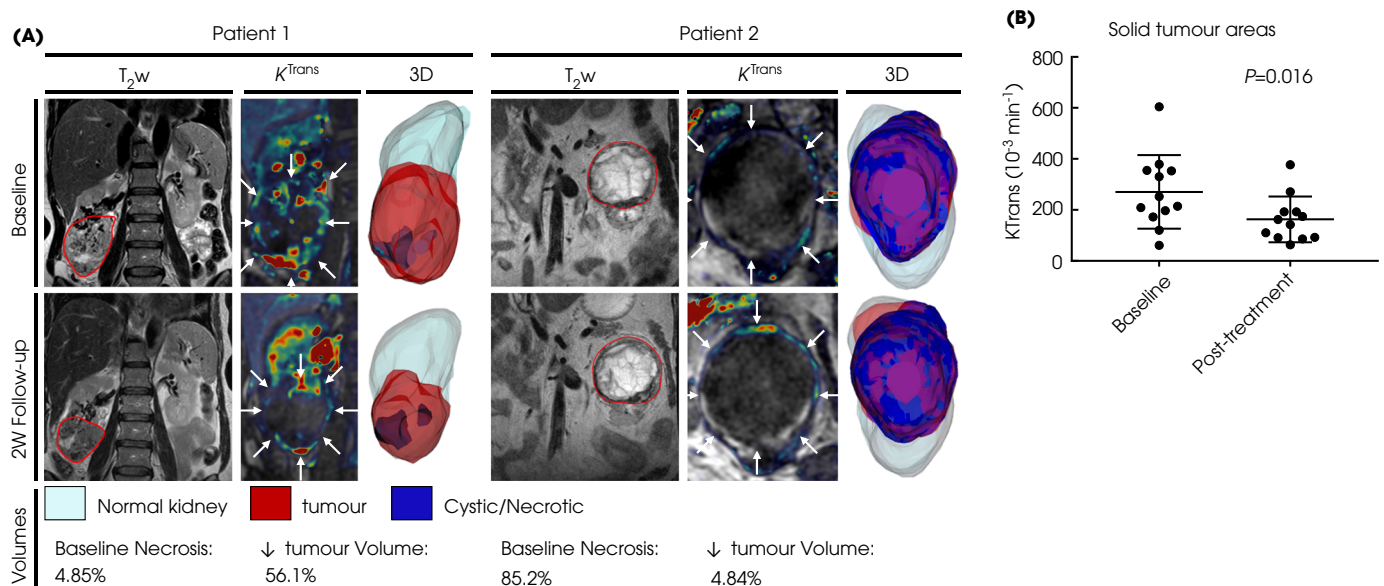
Fig. 2 The molecular effect of pre-surgical sunitinib treatment (for 12 days). Intratumoral necrosis (**A**), proliferation measured using Ki67 (**B**), microvessel density measured using CD31 (**C**), and VEGF-C levels (**F**) were significantly different before and after treatment with 12 days of sunitinib. Pre-treatment microvessel density also correlated with objective response (measured on CT using RECIST version 1.1) (**D**). Pre-treatment VEGF-C levels greater than the median correlated with improved overall survival (**F**). CR, complete response; PR, partial response; SD, stable disease.
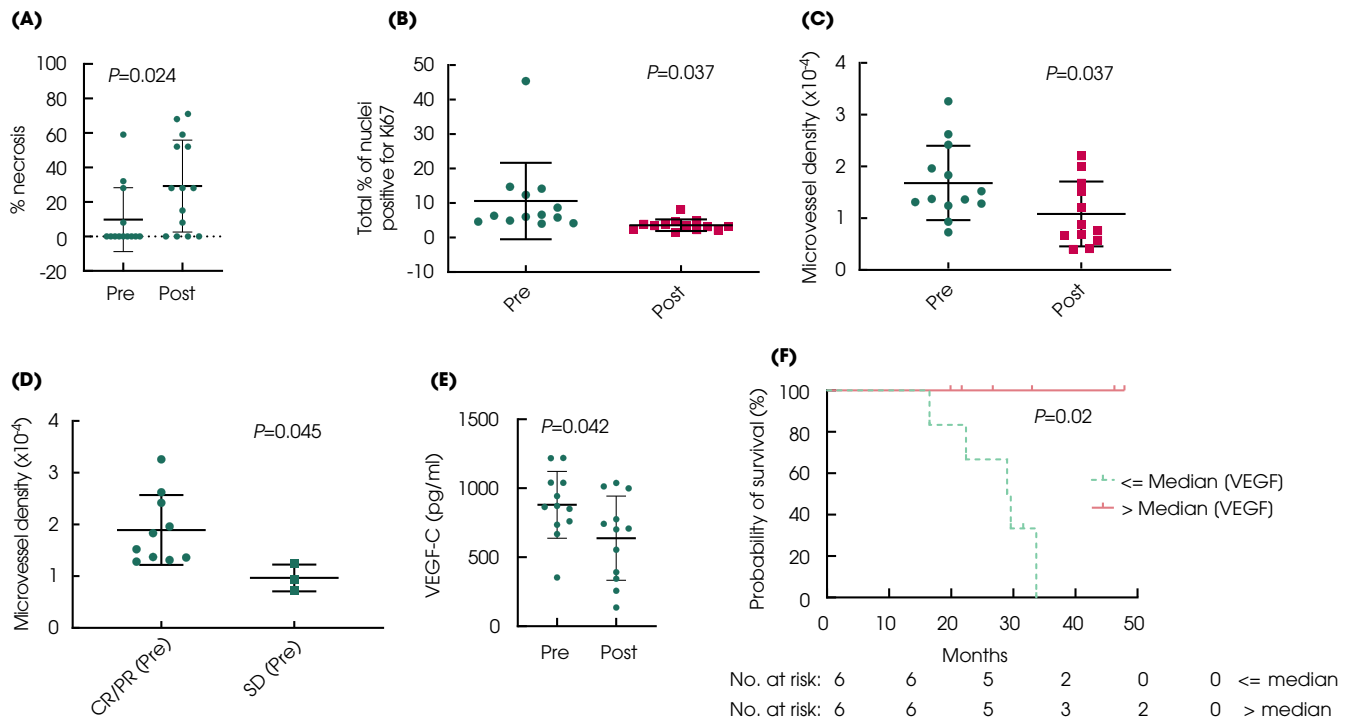
these significantly correlated with OS or ORR. Larger percentage tumour volume reduction after 12 days of sunitinib therapy (measured using MRI) correlated with smaller baseline percentage necrosis (coefficient = −0.51, $P = 0.03$).

Ki67

A total of 13/14 patients had evaluable tissue for analysis of Ki67 using IHC before and after treatment with sunitinib for 12 days. The mean (range) percentage of cells expressing Ki67 significantly decreased after treatment from 21.2 (4.0–45.3)% to 3.6 (1.5–8.2)% ($P = 0.037$; Fig. 2B). The mean (range) change in the percentage of cells expressing Ki67 before and after treatment was 53.7 (15.8–91.7)%. Neither of these significantly correlated with OS or ORR.

Microvessel Density (Measured Using CD31)

A total of 13/14 patients had evaluable tissue for analysis of CD31 using IHC before treatment with 12 days of sunitinib, and 12/14 patients had evaluable tissue for post-treatment analysis. The mean (range) microvessel density significantly decreased after treatment from 1.68 (0.73–3.26) × 10^4 microvessels/unit area to 1.08 (0.40–1.68) × 10^4

microvessels/unit area, respectively ($P = 0.037$; Fig. 2C), but did not significantly correlate with OS. However, pre-treatment microvessel density was significantly higher in patients whose best response was complete response (CR) or partial response (PR), compared to patients whose best response was stable disease (1.83 × 10^4 vs 0.91 × 10^4 microvessels/unit area, respectively; $P = 0.045$; Fig. 2D).

Blood-Based Endpoints

A total of 12/14 patients had evaluable serum samples for VEGF-A and VEGF-C measurement both before and after 12 days of sunitinib therapy. The mean (range) VEGF-A levels before and after treatment were 539 (122–1175) and 885 (229–1590) pg/mL, respectively. The mean (range) difference between VEGF-A levels before and after treatment was 346 (−302 to −1270) pg/mL. Neither baseline nor C1D12 VEGF-A levels, nor the difference between them, significantly correlated with OS.

The VEGF-C levels were significantly reduced after 12 days of sunitinib therapy, at a mean (range) of 880 (353–1219) vs 638 (136–1038) pg/mL ($P = 0.042$; Fig. 2E). The mean (range) difference between VEGF-C levels before and after treatment was −242 (−808 to −28) pg/mL. Whilst the change in VEGF-C levels did not significantly correlate with OS,

median OS was significantly improved in patients with VEGF-C levels ≥median compared with VEGF-C levels ≤median levels (29.3 months vs not reached, respectively; $P = 0.020$; Fig. 2F). This was the same whether levels of VEGF-C were taken before treatment or after treatment.

Discussion

Unfortunately, the primary endpoint of the present study was not reached due to the study closing prematurely as a result of changes to the standard of care treatment for mRCC. However, the study revealed important exploratory data that warrants further study and, within the small sample size, pre-surgical treatment of patients with mRCC with sunitinib was safe. Whilst the study population is small, the demographics of the population are similar to other neoadjuvant studies in mRCC [4–6]. Importantly, consistent with other studies, pre-surgery TKIs did not delay surgery or increase complications intra- or postoperatively [4–6].

Our present study differs from many others in that we gave a short TKI pre-surgical treatment course (12 days vs 6–18 weeks [4,5,13,14]). Given our short treatment course, chosen to devascularise the tumour rather than have any major effect on tumour size, it is interesting that MRI showed a tumour size decrease in all patients, albeit of <10% in the majority of patients. In comparison, others have shown a median tumour volume reduction of 14.4% with 12–14 weeks of preoperative pazopanib [13], and 32% with a 6–12 week course of preoperative sunitinib [5]. This suggests that a prolonged preoperative treatment course may be of limited additional downstaging benefit, although further work is required to explore this given the small numbers in our present study.

However, in our present study, it should be noted that 58.3% and 91.7% of patients treated had a CR/PR and clinical benefit respectively, which is higher than the reported response rates to sunitinib (~17% and 76%, respectively) [10]. A recent pooled study of 461 treatment-naïve patients with their primary tumour *in situ* reported primary tumour response rates of ~28% [15]. Our present higher response rate is likely to reflect patient selection within the small sample size. Notably, newer TKIs such as axitinib, which are more potent inhibitors of the VEGF receptor (VEGFR) may have higher response rates, with one study assessing pre-surgical axitinib reporting a PR rate of 45.8% [16].

Of note, tumours with a higher percentage of solid tumour components at baseline showed a greater reduction in overall tumour volume. Larger percentage tumour volume reduction after 12 days of sunitinib therapy was also correlated with a smaller baseline percentage necrosis on pathology. Additionally, pre-treatment microvessel density was significantly higher in patients whose best response was CR or PR. These findings are important as a previous study

using 4–6 weeks pre-surgical sunitinib found a modest reduction in tumour size in 83% patients, allowing a partial nephrectomy in some tumours where this was not initially an option [5]. Our present study suggests that patients more likely to have tumour volume reductions with sunitinib could potentially be selected based on baseline pathological and MRI characteristics, although this hypothesis requires validation.

The NeoSun aimed to identify early molecular biomarkers of response to sunitinib treatment. We observed that VEGF-C levels above the median (at both baseline and after 12 days treatment) correlated with survival, which may indicate that tumours secreting higher VEGF levels are more likely to respond to sunitinib, consistent with sunitinib's mechanism of action. Others have also found changes in stromal cell-derived factor-1 and soluble VEGFR-1 during neoadjuvant sunitinib treatment to be significantly associated with OS [17]. These biomarkers are regulated by hypoxia and may have a role in guiding sunitinib therapy; tumours with a hypoxic signature are known to have a more aggressive clinical course [18].

Tumour imaging and molecular changes observed were consistent with sunitinib's known mechanism of action. Reduction in K^{Trans} and decreased size of the tumours, were consistent with the reductions in microvessel density (measured by CD31) Ki67, and the increase in necrosis. Decreased microvessel density has also been demonstrated with neoadjuvant sorafenib [19]. One previous study has assessed very early treatment response after 3 and 10 days and found no change in K^{Trans} compared to the baseline examination [26]. However, the significant reduction in K^{Trans} seen in the Neosun after 12 days is in agreement with the reduction observed by Hudson *et al.* [27] after 14 days. Reduction in K^{Trans} has also been observed after 4 and 10 weeks of either sunitinib or pazopanib treatment and change of K^{Trans} between weeks 4 and 10 was associated with the risk of disease progression after 6 months [28].

Baseline K^{Trans} trended towards a positive correlation with volumetric response. However, K^{Trans} was not correlated with PFS in our present study. This may be due to the small sample size in our study. Previous studies have shown a longer PFS in patients treated with sorafenib with a baseline K^{Trans} above the median [29]. Similar findings have been reported for sunitinib, sorafenib and pazopanib, respectively, after longer treatment periods than in the Neosun [27,30,31]. Thus, K^{Trans} may be a useful non-invasive biomarker to confirm biological mechanism of action at an early stage of treatment but requires investigation in larger studies to determine its utility at very early time points as a predictor of longer-term response.

Overall, the NeoSun confirmed that pre-surgical treatment with sunitinib may allow early assessment of treatment

response. Further work is required to establish if any molecular or imaging parameters may robustly predict response to sunitinib (or other more potent TKIs such as axitinib), but both imaging and blood-based biomarkers have been identified that might have potential to aid clinical decision making. We are seeking to validate them within the NAXIVA clinical trial assessing the effect of a short course of neoadjuvant axitinib in locally advanced RCC (NCT03494816).

Acknowledgements

Conflict of Interest

The translational work for this paper was supported by an unrestricted grant to Cambridge Cancer Trials Centre, which we used to support conduct of this study and its associated biomarker work. Sarah J. Welsh, Nicola Thompson, Anne Warren, Andrew N. Priest, Stephan Ursprung, Tristan Barrett, Fulvio Zaccagna, Andrea J. Machin, Wendi Qian, Victoria Ingleson, Antony C.P. Riddick, Stephen Connolly, and Jean Mullin have no disclosures or conflicts of interest to report. James N. Armitage has received speaker fees from Eisai. Kate M. Fife has received research funding from Roche, Merck, Exelixis; conference support from Novartis, Ipsen, EUSA; participated in Advisory Boards for ESAI, IPSEN, Roche, Novartis, Merck, Pfizer, Eusa, BMS; and has received speaker/consultancy fees from BMS, Pfizer, MSD, Sanofi, Esai, IPSEN, Roche, Novartis, Merck, Eusa Pharma. Grant D. Stewart has received educational grants from Pfizer, AstraZeneca, and Intuitive Surgical; consultancy fees from CMR Surgical, Pfizer, and Merck; has participated on Advisory Boards for Merck; and has received honoraria/speaker fees from Merck, Pfizer, EUSA Pharma. Athena Matakidou was an employee of AstraZeneca until December 2020 and is now an employee of GSK; and holds stock in

AstraZeneca and GSK. Timothy G.Q. Eisen has received research support from Pfizer and AstraZeneca; has received meeting support from Roche Genentech; was an employee of AstraZeneca until March 2020 and is now an employee of Roche; and holds stock in AstraZeneca and Roche. Ferdia A. Gallagher has research support from CRUK, NIHR BRC; GE Healthcare, and GSK; and consulting fees from AstraZeneca.

References

1 Hock LM, Lynch J, Balaji KC. Increasing incidence of all stages of kidney cancer in the last 2 decades in the United States: an analysis of surveillance, epidemiology and end results program data. *J Urol* 2002; 167: 57–60

2 Méjean A, Ravaud A, Thezenas S et al. Sunitinib alone or after nephrectomy in metastatic renal-cell carcinoma. *N Engl J Med* 2018; 379: 417–27

3 Albiges L, Powles T, Staehler M et al. Updated European Association of Urology guidelines on renal cell carcinoma: immune checkpoint inhibition is the new backbone in first-line treatment of metastatic clear-cell renal cell carcinoma. *Eur Urol* 2019; 76: 151–6

4 De Bruijn RE, Mulders P, Jewett MA et al. Surgical safety of cytoreductive nephrectomy following sunitinib: results from the multicentre, randomised controlled trial of immediate versus deferred nephrectomy (SURTIME). *Eur Urol* 2019; 76: 437–40

5 Lane BR, Derweesh IH, Kim HL et al. Presurgical sunitinib reduces tumor size and may facilitate partial nephrectomy in patients with renal cell carcinoma. *Urol Oncol* 2015; 33: 112.e15–21

6 Rini BI, Garcia J, Elson P et al. The effect of sunitinib on primary renal cell carcinoma and facilitation of subsequent surgery. *J Urol* 2012; 187: 1548–54

7 Thomas AA, Rini BI, Lane BR et al. Response of the primary tumor to neoadjuvant sunitinib in patients with advanced renal cell carcinoma. *J Urol* 2009; 181: 518–23

8 Pilié PG, Jonasch E. Systematic review: perioperative systemic therapy for metastatic renal cell carcinoma. *Kidney Cancer* 2017; 1: 57–64

9 Grant M, Szabados B, Kuusk T, Powles T, Bex A. Cytoreductive nephrectomy: does CARMENA (Cancer du Rein Metastatique Nephrectomie et Antiangiogéniques) change everything? *Curr Opin Urol* 2020; 30: 36–40

10 Gore ME, Szczylik C, Porta C et al. Safety and efficacy of sunitinib for metastatic renal-cell carcinoma: an expanded-access trial. *Lancet Oncol* 2009; 10: 757–63

11 Eisenhauer EA, Therasse P, Bogaerts J et al. New response evaluation criteria in solid tumours: revised RECIST guideline (version 1.1). *Eur J Cancer* 2009; 45: 228–47

12 Dindo D, Demartines N, Clavien PA. Classification of surgical complications: a new proposal with evaluation in a cohort of 6336 patients and results of a survey. *Ann Surg* 2004; 240: 205–13

13 Powles T, Sarwar N, Stockdale A et al. Safety and efficacy of pazopanib therapy prior to planned nephrectomy in metastatic clear cell renal cancer. *JAMA Oncol* 2016; 2: 1303–9

14 Powles T, Blank C, Chowdhury S et al. The outcome of patients treated with sunitinib prior to planned nephrectomy in metastatic clear cell renal cancer. *Eur Urol* 2011; 60: 448–54

15 Bossé D, Lin X, Simantov R et al. Response of primary renal cell carcinoma to systemic therapy. *Eur Urol* 2019; 76: 852–60

16 Karam JA, Devine CE, Urbauer DL et al. Phase 2 trial of neoadjuvant axitinib in patients with locally advanced nonmetastatic clear cell renal cell carcinoma. *Eur Urol* 2014; 66: 874–80

17 Mauge L, Mejean A, Fournier L et al. Sunitinib prior to planned nephrectomy in metastatic renal cell carcinoma: angiogenesis biomarkers

predict clinical outcome in the prospective phase II PREINSUT trial. *Clin Cancer Res* 2018; 24: 5534–42

18 **Beuselinck B, Job S, Becht E et al**. Molecular subtypes of clear cell renal cell carcinoma are associated with sunitinib response in the metastatic setting. *Clin Cancer Res* 2015; 21: 1329–39

19 **Desar IME, Stillebroer AB, Oosterwijk E et al**. 111In-bevacizumab imaging of renal cell cancer and evaluation of neoadjuvant treatment with the vascular endothelial growth factor receptor inhibitor sorafenib. *J Nucl Med* 2010; 51: 1707–15

20 **Rini BI, Plimack ER, Takagi T et al**. A phase II study of pazopanib in patients with localized renal cell carcinoma to optimize preservation of renal parenchyma. *J Urol* 2015; 194: 297–303

21 **Bigot P, Fardoun T, Bernhard JC et al**. Neoadjuvant targeted molecular therapies in patients undergoing nephrectomy and inferior vena cava thrombectomy: is it useful? *World J Urol* 2014; 32: 109–14

22 **Harshman LC, Yu RJ, Allen GI, Srinivas S, Gill HS, Chung BI**. Surgical outcomes and complications associated with presurgical tyrosine kinase inhibition for advanced renal cell carcinoma (RCC). *Urol Oncol* 2013; 31: 379–85

23 **Hellenthal NJ, Underwood W, Penetrante R et al**. Prospective clinical trial of preoperative sunitinib in patients with renal cell carcinoma. *J Urol* 2010; 184: 859–64

24 **Silberstein JL, Millard F, Mehrazin R et al**. Feasibility and efficacy of neoadjuvant sunitinib before nephron-sparing surgery. *BJU Int* 2010; 106: 1270–6

25 **Tofts PS, Brix G, Buckley DL et al**. Estimating kinetic parameters from dynamic contrast-enhanced T(1)-weighted MRI of a diffusable tracer: standardized quantities and symbols. *J Magn Reson Imaging* 1999; 10: 223–32

26 **Desar IM, ter Voert EG, Hambrock T et al**. Functional MRI techniques demonstrate early vascular changes in renal cell cancer patients treated with sunitinib: a pilot study. *Cancer Imaging* 2012; 11: 259–65

27 **Hudson JM, Bailey C, Atri M et al**. The prognostic and predictive value of vascular response parameters measured by dynamic contrast-enhanced-CT, -MRI and -US in patients with metastatic renal cell carcinoma receiving sunitinib. *Eur Radiol* 2018; 28: 2281–90

28 **Zhong J, Palkhi E, Buckley DL et al**. Feasibility study on using dynamic contrast enhanced MRI to assess the effect of tyrosine kinase inhibitor therapy within the STAR trial of metastatic renal cell cancer. *Diagnostics* 2021; 11: 1302

29 **Flaherty KT, Rosen MA, Heitjan DF et al**. Pilot study of DCE-MRI to predict progression-free survival with sorafenib therapy in renal cell carcinoma. *Cancer Biol Ther* 2008; 7: 496–501

30 **Hahn OM, Yang C, Medved M et al**. Dynamic contrast-enhanced magnetic resonance imaging pharmacodynamic biomarker study of sorafenib in metastatic renal carcinoma. *J Clin Oncol* 2008; 26: 4572–8

31 **Sweis RF, Medved M, Towey S et al**. Dynamic contrast-enhanced magnetic resonance imaging as a pharmacodynamic biomarker for pazopanib in metastatic renal carcinoma. *Clin Genitourin Cancer* 2017; 15: 207–12

Correspondence: Sarah Welsh, Department of Oncology, Cambridge University Hospitals NHS Foundation Trust, Box 193, Hills Road, Cambridge CB2 0QQ, UK.

e-mail: sjw236@cam.ac.uk

Abbreviations: CD31, cluster of differentiation; CONSORT, Consolidated Standards of Reporting Trials; CR, complete response; 2D, two-dimensional; 3D, three-dimensional; DCE-MRI, dynamic contrast-enhanced MRI; ETL, echo train length; FoV, field of view; FSPGR, fast spoiled gradient-echo; IHC, immunohistochemistry; K^{Trans}, transfer constant; mRCC, metastatic RCC; ORR, overall response rate; OS, overall survival; PFS, progression-free survival; PR, partial response; RECIST, Response Evaluation Criteria In Solid Tumors; TKI, tyrosine kinase inhibitor; TE, echo time; TR, repetition time; TT, tumour thrombus; VEGF-C, vascular endothelial growth factor C; VEGFR, vascular endothelial growth factor receptor.

Supporting Information

Additional Supporting Information may be found in the online version of this article:

Fig. S1. NeoSun trial schema.
Fig. S2. NeoSun CONSORT diagram.
Table S1. Summary of toxicities.
Table S2. Surgical outcomes and complications.
Appendix S1. Supplementary methods and results.